Measurement of deuteron-deuteron total cross sections in the incident momentum range 1.5–4.0 GeV/c

T. Kishida, K. Ishikawa, M. Kuze, F. Sai,* and S. S. Yamamoto
Department of Physics, University of Tokyo, Tokyo 113, Japan

T. Maki
Department of Physics, University of Occupational and Environmental Health, Kitakyusyu, Fukuoka-ken 807, Japan

I. Arai, A. Manabe, and H. Nunokawa†
Institute of Physics, University of Tsukuba, Tsukuba, Ibaraki-ken 305, Japan

H. Koiso and T. Tsuboyama
National Laboratory for High Energy Physics, Tsukuba, Ibaraki-ken 305, Japan
(Received 26 July 1989)

We have made the first systematic precision measurement of the deuteron-deuteron total cross sections at 12 incident momenta in the range of 1.5–4.0 GeV/c on a proton synchrotron. The data were obtained by means of the transmission method covering the momentum transfer squared range of 0.001 to 0.009 (GeV/c)^2 at each momentum. Our data show no anomalous structure in the excitation function and are in good agreement with Glauber model calculations including the effect of the Fermi motion of the nucleons in the deuteron except at 1.5 GeV/c, where the datum is lower than the calculated value.

I. INTRODUCTION

The deuteron is the simplest system of nucleons. It is a loosely bound state of a proton and a neutron, the binding energy of which is 2.2 MeV, and its wave function has been well investigated. The accumulated knowledge of the deuteron enables us to make quantitative analysis of scattering processes with deuteron beams theoretically. The deuteron-deuteron reaction is, therefore, important and fundamental in the study of the nucleus-nucleus system. Experimental study of this reaction provides a test of the features predicted by multiple nuclear scattering theories for cases where both the projectile and target are composite.

Theoretical studies of nucleus-nucleus scattering have been actively carried out during the last three decades as extensions of nucleon-nucleus multiple scattering theories. In the intermediate energy region the multiple scattering theory of Glauber[1,2] is a standard tool to describe nucleon-nucleus reactions quantitatively. With the aid of this method we can calculate nucleon-nucleus scattering amplitudes using the data of nucleon-nucleon scattering amplitudes (N-N amplitudes) and the nuclear density distribution without the full knowledge of the interaction between nucleons such as the exact form of the potential. An extension of the Glauber model to the nucleus-nucleus system was carried out first by Franco, who calculated the deuteron-deuteron scattering amplitudes (d-d amplitudes).[3] Though d-d scattering is the simplest example of the collision between two nuclei, the number of terms and the order of integration in the d-d amplitudes are about three to four times larger than those in the p-d amplitudes. It is no longer realistic to expect that the exact calculation of the Glauber model can be made in cases where both projectile and target consist of more than two nucleons. Hence the Glauber calculations of nucleus-nucleus amplitudes have been usually made with some approximations.[4–10]

While a lot of theoretical studies exist, there are only a few d-d total cross section data in the deuteron momentum range of 1.5–4.0 GeV/c in spite of the fact that the total cross section is one of the most important observables in the study of scattering processes. In the intermediate momentum range of 1.5–4.0 GeV/c, which is the range covered by our experiment, there are a datum at 3.0 GeV/c by Debaisieux *et al.*,[11] data at 1.50, 1.75, and 2.12 GeV/c by Goshaw *et al.*,[12] and a datum at 3.1 GeV/c by Jaros *et al.*[13] The datum by Debaisieux *et al.* is much lower than both the impulse approximation prediction $2\times(\sigma_{pp}+\sigma_{np})$ and the Glauber prediction. The data by Goshaw *et al.* agree with the impulse approximation prediction as in the case of p-d total cross sections in this energy region.[14–17] And the datum by Jaros *et al.* agreed with a simplified version of the Glauber theory. To summarize the above, there are no systematic data of d-d total cross sections, and the few data points that do exist have large errors and some disagree with one another.

The main aim of this experiment is to make the first systematic high-precision measurement of the d-d total cross sections as a function of incident momentum to see if there is any unexpected anomaly in their behavior, and if not, to compare them with theoretical calculations to check the validity of the Glauber model. The incident deuteron momentum range of 1.5–4.0 GeV/c chosen for this experiment covers the region where the single pion

production threshold opens and the total cross section increases rapidly with momentum due to the increase of the pion production cross sections of the N-N interactions. This momentum range was also chosen for the following reasons: (1) A good N-N phase shift analysis[18] is available in the equivalent nucleon momentum range; (2) the low energy limit, where the simple calculations of the Glauber model are no longer valid, was reported in the measurements of N-nucleus scattering in the equivalent nucleon momentum range.[16,17,19].

The measurement of the total cross section is adequate to check the validity of the theory quantitatively, and it is insensitive to some ambiguities in what goes into theoretical calculation, while the differential cross section is sensitive to them. (For example, we can smear the diffraction patterns in elastic differential cross section either by using N-N amplitudes with a momentum transfer dependent phase,[20] by including the effect of Coulomb interaction,[21] or by including the D-wave contribution of the deuteron.) However, it is necessary to perform high-precision measurements in order to meaningfully investigate the effects of multiple scattering using data on total cross sections. The d-d total cross sections, for instance, must be measured to at least a 1% accuracy (about 1.5 mb) before it is possible to measure the cross section defects $\Delta\sigma = 2\times(\sigma_{pp}+\sigma_{np})-\sigma_{dd}$ to a 10% accuracy. Our experiment is intended to obtain more accurate data than that by Jaros *et al.* and to study the energy dependence of the total cross sections systematically.

II. EXPERIMENTAL ARRANGEMENT

The data were obtained by means of the transmission method using the secondary beam from an internal target of the 12-GeV proton synchrotron at the National Laboratory for High Energy Physics (KEK). The experiment was performed at the incident deuteron momenta of 1.5, 2.0, 2.2, 2.4, 2.6, 2.8, 3.0, 3.2, 3.4, 3.6, 3.8, and 4.0 GeV/c. The detector system consisted of time of flight counters $S1$, $S2$, and $S3$, an annular-shaped beam defining anticounter A; a transmission counter array $T1$-$T7$, and four multiwire proportional chambers (MWPC's) $W1$-$W4$. A liquid deuterium target was used. A schematic diagram of the experimental arrangement is shown in Fig. 1.

A. Deuteron beam

As shown in Fig. 1, the secondary particles were produced at the internal target (IT) and the positively charged particles were transported to an intermediate focus where a momentum slit and trigger counter $S1$ were located. The beam line magnets after this focus were tuned so that the beam should be refocused onto the experimental target. The momentum bite depends on the width of the momentum slit and was estimated to be less than 1% in our experiment. The yield of deuterons was 0.5–0.6 % of all positively charged particles for each incident momentum. The deuterons were assumed to be unpolarized in the experiment.

B. Liquid-deuterium target

The target system consisted of two target cells, a vacuum chamber, a refrigeration unit, and a monitor-control system. The system was almost the same as that described by Sumiyoshi, Suzuki, and Nakamura,[22] except for the target cells[23] and the monitor-control system.[24]

Two identical target cells, one filled with liquid deuteri-

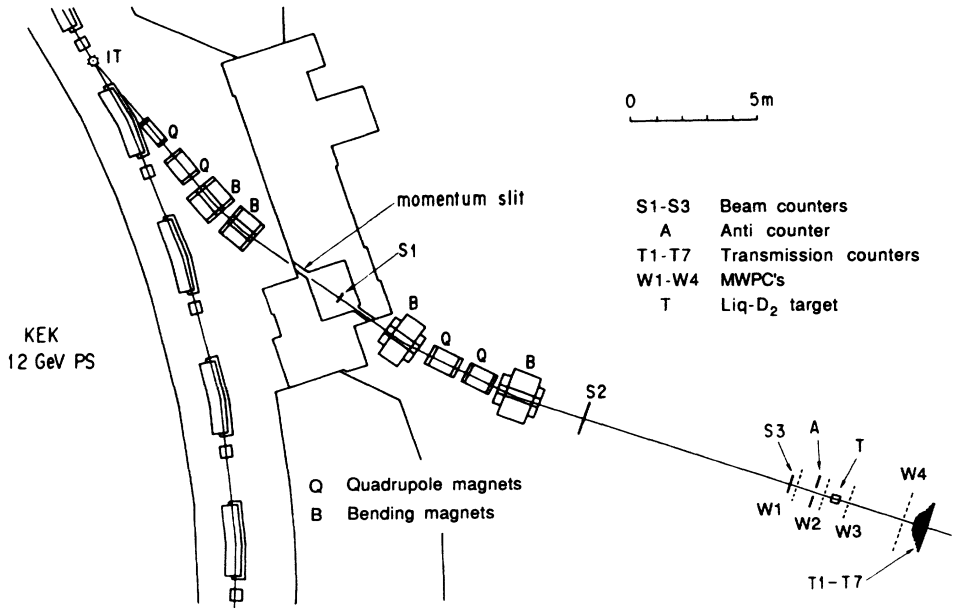

FIG. 1. Configuration of the beam line elements.

um and the other left empty, were used in the transmission experiment. Each target cell was cylindrical in shape and was 20 cm long and 6 cm in diameter. The target length was measured accurately under the experimental condition and found to be 201.4±0.1 mm long. The endcaps of the target cells were made of 188-μm-thick cup-shaped mylar with a central bulge and were glued to the mylar cylinders with adhesive resin.

The difference between the atmospheric pressure and the vapor pressure of liquid deuterium above the liquid surface was always monitored and controlled to be constant at 0.041±0.001 kg/cm^2 with a heater attached to the condenser chamber of the refrigerator.[24] The fluctuation of the vapor pressure was, therefore, caused by the fluctuation in the atmospheric pressure, which we assumed to be at most 0.036 kg/cm^2. Consequently, the vapor pressure of liquid deuterium was controlled to 1.075±0.036 kg/cm^2, which meant that the temperature of liquid deuterium was controlled to 23.8±0.1 K (Ref. 25) and the density to 0.1626±0.0003 g/cm^3 (Ref. 26).

C. Trigger counters

The deuterons in the beam were selected first with the trigger system during on-line data taking, and second with the time-of-flight data obtained from the trigger counters in the off-line analysis. The trigger counter system consisted of three time of flight counters $S1$, $S2$, and $S3$, and an annular shaped beam defining anticounter A. The trigger logic was $S1 \cdot S3 \cdot \overline{A}$. The deuterons in the beam were selected by opening a narrow coincidence gate of about 8 ns at the time corresponding to the deuteron time of flight between $S1$ and $S3$, which were separated by a distance of 19 m. Events acquired with this trigger still contained some spurious coincidence signals, which amounted to as much as 40% in the worst case. This is because the number of deuterons was about 0.6% of that of all positively charged particles in the beam, and the deuteron counting rate was about 400 Hz, while the single counting rates of $S1$ and $S3$ were about 130 and 80 kHz, respectively. However, the spurious coincidence events were eliminated by using the information on the time of flight between $S2$ and $S3$ separated by 8.5 m in the off-line analysis. Figure 2(a) is a histogram of the time of flight between $S2$ and $S3$ at 4.0 GeV/c, and it shows the fact that spurious coincidence signals were caused by the high counting rates of protons and pions. Figure 2(b) shows a scatter plot of the time of flight between $S1$ and $S3$ and that between $S2$ and $S3$, where the deuterons are seen to form a clear cluster. Only the events within the arrows indicated in Fig. 2(a) were accepted. A further cut was made on the time of flight between $S1$ and $S3$ as indicated by the vertical dotted lines in Fig. 2(b). The purity of the beam after the off-line cut was evaluated to be more than 99.9%.

The method of time of flight, however, could not eliminate contamination by the breakup protons which came from the deuterons broken up in the material in the beam line after the last beam line magnet, since they have the same velocity as the deuterons. They will not have any structure in the analog-to-digital converter (ADC) and time-to-digital converter (TDC) spectra, and we calculated the contamination of the deuteron beam by the breakup protons with the help of experimental data on d-p breakup cross sections,[27] and estimated it to be less than 0.3%.

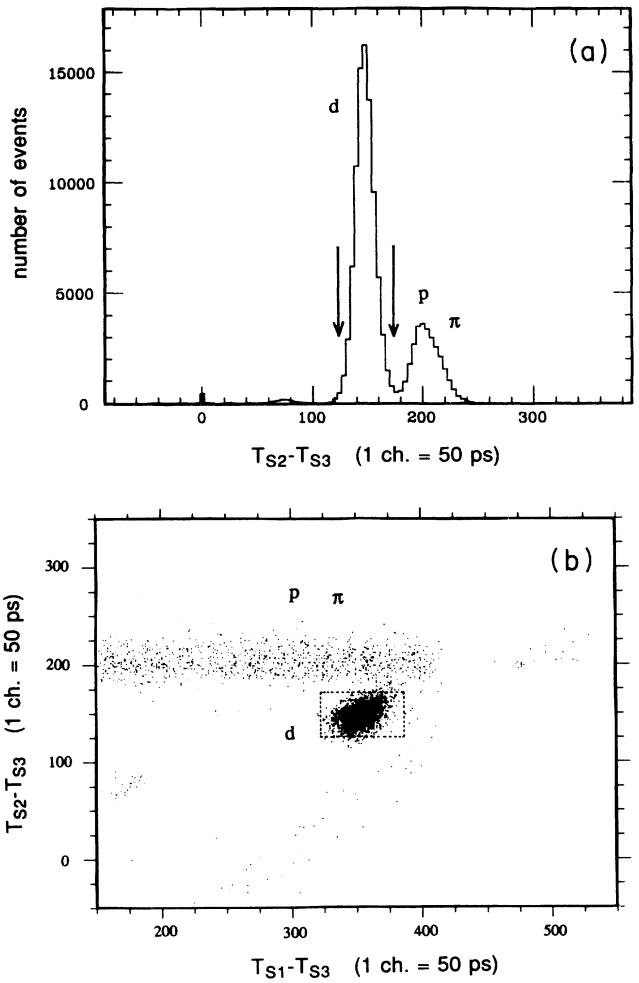

FIG. 2. (a) Time-of-flight (TOF) spectrum between $S2$ and $S3$ (T_{S2}-T_{S3}) at 4.0 GeV/c, and (b) scatter plot between TOF($S1$-$S3$) and TOF($S2$-$S3$) at 4.0 GeV/c. In both figures the time axes are in units of TDC channel number (ch.). It can be seen that the deuterons form a clear cluster even in the case of 4.0 GeV/c, where the difference in the time of flight is the smallest.

D. Transmission counters

The scattered particles from the target were detected by seven 3-mm-thick plastic scintillation transmission disk counters. They had diameters of 5.0, 6.5, 8.0, 9.5, 10.5, 12.5, and 15.0 cm. The concentric disk counter system was mounted on a movable platform together with MWPC $W4$. The center of the counter array was placed on the beam axis to an accuracy of ±1.0 mm. The distance between the target center and the counter array was such that at each incident momentum it covered the momentum transfer squared in the range of $0.001 \leq -t \leq 0.009$ (GeV/c)^2. The hits in the disk counters by scattered particles were recognized by using the data on their ADC and TDC in the off-line analysis.

E. Multiwire proportional chambers

Four MWPC's, $W1-W4$,[28] were used for the reconstruction of the incident and scattered particle trajectories. The spacing of both anode and cathode wires was 2 mm. MWPC's $W1-W3$ had a sensitive region of about 10×10 cm^2 and $W4$ had a sensitive region of about 20×20 cm^2. A gas mixture consisting of 71.5% argon, 25% isobutane, 3.3% methylal, and 0.25% freon was used. A negative high voltage of 4.7 kV was applied to the cathode wires.

Data from MWPC's $W1$ and $W2$ were used in the off-line analysis to limit the size of the incident beam within a diameter of 3 cm at the positions of $W1$ and $W2$ and the transmission counter array by extrapolating the incident trajectories. Data from MWPC's $W3$ and $W4$ were also used in the analysis to measure the acceptances of the transmission counters, the details of which will be described in Sec. III B. MWPC $W4$ was also used during the experiment for monitoring the beam profile at the transmission counter array, the center of which had to be placed on the beam axis.

F. Electronics

The electronics used in this experiment consists of three parts: the trigger logic, the CAMAC system, and the data-acquisition system. A schematic diagram of the electronics is shown in Fig. 3. The signals from $S1$, $S3$, and A were transmitted to discriminators, which shaped the signals from $S1$ and $S3$ into typically 10-ns-wide pulses, and the signals from A into 50-ns-wide pulses. The pulse from $S1$ was transmitted to a variable delay. The timing of the coincidence among $S1$, $S3$, and A was adjusted to the deuteron time of flight with this delay at each momentum. The trigger signal thus produced was used to gate the ADC, TDC, and the memory modules of the MWPC's. The signals from each plastic scintillation counter and each MWPC were converted into digital data with CAMAC modules. By using two minicomputers PDP-11/34 and CCS-11 we acquired the following data for each event: the ADC data of counters $S1$, $S2$, $S3$, A, and $T1-T7$, the TDC data of the counters except for the anticounter A, and the MWPC hit patterns digitized by the MWPC memory modules.

G. Data-taking procedure

The data taking was performed in two steps at each momentum: a target-full run and a target-empty run, for which the dummy target was used. After all the off-line cuts described in Secs. II C and II E had been made, approximately 700 000 events were obtained with the liquid-deuterium target and 300 000 events with the dummy target at each momentum.

In order to check the systematic effects, we performed "cross checks" and "all-trigger runs." As mentioned earlier, the transmission counter array was usually placed so that it covered the momentum transfer squared range of 0.0010—0.0090 (GeV/c)^2. But we also performed a measurement at 2.0 GeV/c in such a way that the counter array covered the range of 0.0004–0.0035 (GeV/c)^2, and a measurement at 4.0 GeV/c in the range of 0.0016–0.0140 (GeV/c)^2 by changing the distance between the target center and the counter array in addition to the regular runs. In this way, we could look for the possible systematic effects caused by each counter and the validity of the method for corrections and extrapolations to be described in Sec. III. We also performed an all-trigger run at each momentum by opening a wide coincidence gate and accepting all positively charged particles. Data from an all-trigger run were used for the study of the characteristics of the spurious coincidence by protons and pions manifested in their ADC and TDC structures.

III. ANALYSIS AND CORRECTION

A. Transmission method

The transmission method is well known as a technique for measuring nuclear total cross sections and is discussed in several articles[14,29–31] and will be described

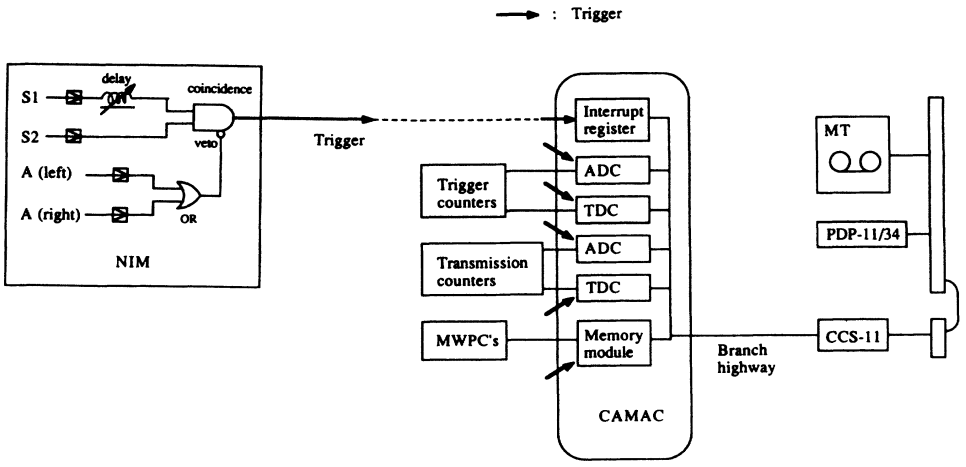

FIG. 3. Schematic diagram of the electronics.

only briefly. If M is the number of incident particles, N_i the number of particles detected by the transmission counter T_i, and σ_i the partial cross section, which is the cross section for beam particles to be scattered outside the counter T_i, then the transmission N_i/M is related to the partial cross section by the following formula:

$$\frac{N_i}{M}=\varepsilon \exp(-n\sigma_i) ,$$

where n is the number of scatters per unit area in the target and ε is the background absorption due to other scatterers in the beam line. The transmission is measured in the target-full run ($n\neq 0$) and in the target-empty run ($n=0$), and then the partial cross section can be extracted from their ratio

$$\sigma_i=-\frac{1}{n}\ln\frac{(N_i/M)_{\text{full}}}{(N_i/M)_{\text{empty}}} .$$

The partial cross section is related to the differential cross section as follows:

$$\sigma_i=\int_0^{t_{\max}}[1-G_i(t)]\left|\frac{d\sigma}{dt}\right|dt ,$$

where $G_i(t)$ is the acceptance function of the transmission counter T_i to be described later and $t\equiv|t|$. The acceptances of the transmission counters are not step functions because of the beam size, the beam divergence, the target length, and position dependence of the efficiency of the counters.

In order to obtain the total cross section σ_{tot} from a set of partial cross sections σ_i, first we correct all the partial cross sections for the single Coulomb, multiple Coulomb, and Coulomb-nuclear interference contributions, which can be calculated theoretically. For example, the correction due to single Coulomb scattering having the differential cross section $(d\sigma/dt)_C$ is defined as

$$\Delta\sigma_C\equiv\int_0^{t_{\max}}[1-G_i(t)]\left|\frac{d\sigma}{dt}\right|_C dt .$$

The Coulomb-nuclear interference and multiple Coulomb terms are also defined in the same way as the single Coulomb term. We then extrapolate the corrected data to zero solid angle using a simple function. The extrapolation procedure is justified by the fact that, in the momentum transfer squared range of our measurement, the nuclear differential cross section has no structure and is almost linear in it.

B. Acceptance

In our experiment, the acceptance was defined as the efficiency of a disk counter as a function of t. It was calculated with the data from the two beam defining MWPC's ($W1$ and $W2$) and the two downstream MWPC's ($W3$ and $W4$) using only those events for which the beam and scattered trajectories were unambiguously defined by the MWPC's. The scattering vertex and the momentum transfer squared to the scattered particle were calculated from these trajectories. Figure 4 shows a scatter plot between the momentum transfer squared and the vertex point (the coordinate along the beam line) in a target-full run with liquid deuterium and that in a target-empty run. It clearly shows scattering by liquid deuterium and the MWPC's $W2$ and $W3$. We also limited the vertex points to the region shown by the arrows in Fig. 4 to reject the background events. A hit signal associated with a set of beam and scattered trajectories identified by the MWPC's, as described above, was looked for in each disk counter. This hit corresponds to a definite value of t as determined by the trajectories, and we plotted a histogram of the number of hits against t for each disk counter in intervals of 1.25×10^{-4} $(\text{GeV}/c)^2$. The number of hits in a given t interval divided by the number of scattered trajectories for the same interval gives the efficiency of this disk counter for this value of t.

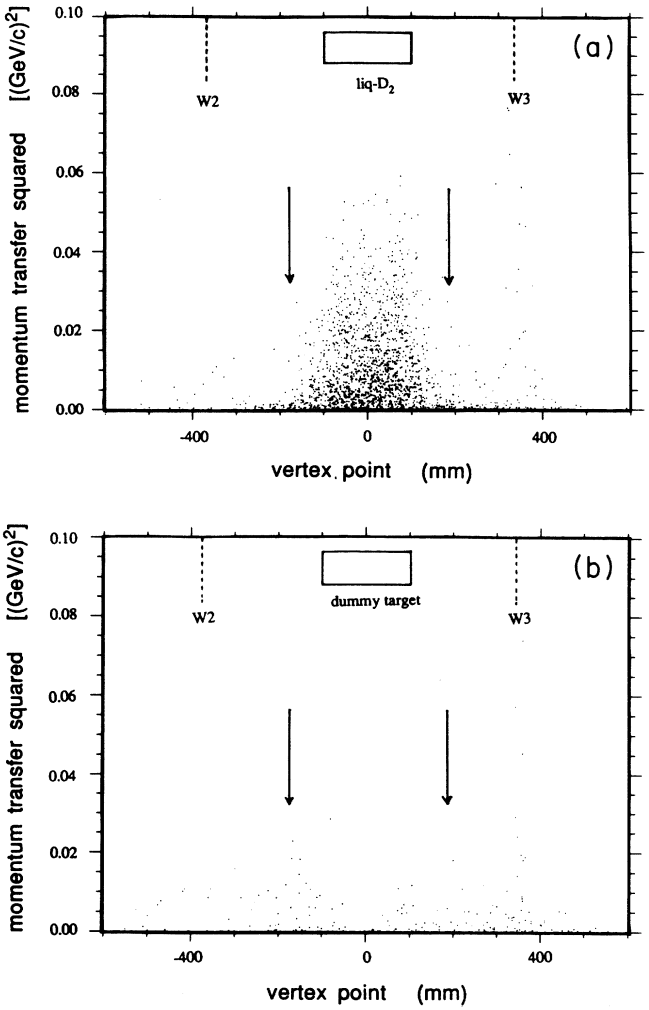

FIG. 4. (a) Scatter plot between the momentum transfer squared and the vertex point for a target-full run with liquid deuterium, and (b) the same for a target-empty run. The arrows in the figures represent the limits of the cut on the scattering point.

Figure 5 shows the acceptances of all seven counters at 4.0 GeV/c. The bin width of 1.25×10^{-4} $(\text{GeV}/c)^2$ was chosen so that it was as large as the size of the uncertain-

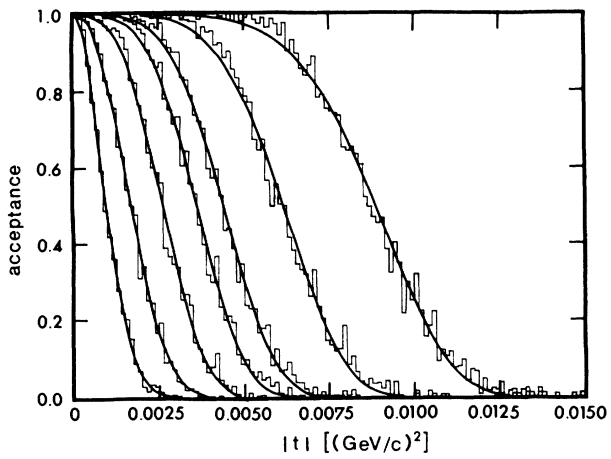

FIG. 5. Acceptance of the disk counters in the d-d experiment at 4.0 GeV/c. The measured values are shown by the histograms and the fitted values by the solid curves. The left-most and right-most histograms correspond to the smallest and largest transmission counters, respectively.

ties in t caused by the spatial resolution of the MWPC's and by multiple scattering by air. The experimental acceptance of the ith counter was fitted to the form

$$G_i(t)=\exp[-(t/Q_i)^{\delta_i}] ,$$

where Q_i and δ_i were the fitting parameters. The fit to this function was good for all transmission counters. The fitted functions are shown as the solid curves in Fig. 5.

C. Single and multiple Coulomb correction

As described in the previous section, the Coulomb contribution had to be calculated in an integral form. The contribution to the integral from backward scattering was usually very small because the angular distribution of Coulomb scattering falls rather fast with increasing scattering angle. On the other hand, the contribution from forward scattering was very important because we calculated the Coulomb contribution using the acceptance functions, which were not exactly unity [e.g., $1-G_i(t)\neq 0$] even at rather small angles.

The calculation of single Coulomb scattering was made exactly with a screened Coulomb potential by using the statistical distribution of the 1s electron. The result is as follows:

$$\left[\frac{d\sigma}{dt}\right]_C=4\pi\left[\frac{\alpha}{\beta}\right]^2\frac{[2(2/a_0)^2+t]^2}{[(2/a_0)^2+t]^4}F_d^4(t) ,$$

where α is the fine-structure constant ($\approx\frac{1}{137}$), a_0 is the Bohr radius ($\approx 5.29\times 10^4$ fm), β is the laboratory velocity of the incident deuteron, and $F_d(t)$ is the electric form factor of the deuteron. The charge distribution was calculated with a wave function obtained by using the Paris potential.[32,33]

The angular distribution of multiple Coulomb scattering has been calculated by several authors[31,34–37] as $f(\theta)\theta\, d\theta$, the probability for the incident particle to be scattered into an angular interval $[\theta,\theta+d\theta]$. To evaluate this probability, Molière[36] defined a new variable η by

$$\eta=\frac{\theta}{\chi_c B^{1/2}} ,$$

where

$$\chi_c^2=\frac{4\pi n\alpha^2}{k^2\beta^2} ,$$

$$\frac{e^B}{B}\equiv\frac{\chi_c^2}{\chi_a'^2} ,$$

and χ_a' is the screening angle $\chi_a'=1.206/(ka_0)$ for the case using a deuterium target and a deuteron beam having the laboratory momentum of k. (The definition of B was somewhat modified by the Fano; see Ref. 38.) Then the probability function is expanded in a series in $1/B$, which gives

$$f(\theta)\theta\, d\theta=\eta\, d\eta\left[f_0(\eta)+\frac{1}{B}f_1(\eta)+\frac{1}{B^2}f_2(\eta)+\cdots\right] ,$$

where

$$f_m(\eta)=\frac{1}{m!}\int_0^\infty u\, du\, J_0(\eta u)\times\exp(-\tfrac{1}{4}u^2)[\tfrac{1}{4}u^2\ln(\tfrac{1}{4}u^2)]^m .$$

To obtain an accuracy of 1% only the first three terms are needed ($m=0,1,2$). We calculated the function $f_m(\eta)$ by using asymptotic formulas.[34,37]

We can describe the multiple Coulomb differential cross section $(d\sigma/dt)_{\text{multi}}$ by using this probability. First, the probability to be scattered outside the angle θ can be given as follows:

$$\int_\theta^\infty f(\theta')\theta' d\theta'=1-\exp[-n\sigma(\theta)] ,$$

where

$$\sigma(\theta)\equiv\int_t^{t_{\max}}\left[\frac{d\sigma}{dt'}\right]_{\text{multi}}dt' .$$

Then, we obtained the differential cross section of multiple Coulomb scattering by differentiating $\sigma(\theta)$ with respect to t

$$\left[\frac{d\sigma}{dt}\right]_{\text{multi}}=\frac{1}{n}\frac{1}{2k^2}f(\theta)\Big/\left[1-\int_\theta^\infty f(\theta')\theta' d\theta'\right] .$$

Since this differential cross section includes the single Coulomb contribution, we redefined it as follows:

$$\left[\frac{d\sigma}{dt}\right]_{\text{multi}}=\frac{1}{n}\frac{1}{2k^2}f(\theta)\Big/\left[1-\int_\theta^\infty f(\theta')\theta' d\theta'\right]-\left[\frac{d\sigma}{dt}\right]_C ,$$

where $(d\sigma/dt)_C$ is the differential cross section for a single Coulomb scattering. The resulting multiple Coulomb differential cross section is large at very small angles and falls more rapidly than the single Coulomb term.

D. Coulomb-nuclear interference correction

The Coulomb-nuclear interference contribution is defined as the interference between the single Coulomb amplitude and the nuclear elastic amplitude. To see this, we must consider only the elastic amplitude because inelastic Coulomb scattering can be negligible.

The elastic amplitude is given as

$$f_{\text{elastic}} = f_{N_{\text{el}}} + f_{\text{C}} ,$$

where f_{C} is the single Coulomb amplitude and $f_{N_{\text{el}}}$ is the "Coulomb corrected" nuclear amplitude. This correction is caused by the radiative correction to the nuclear amplitude. Locher reported that the effect of the radiative correction changes the nuclear amplitude only in phase.[39] Therefore we can describe the elastic amplitude in a simple addition form.

Since the elastic differential cross section is $|f_{\text{elastic}}|^2$, the Coulomb-nuclear interference contribution is

$$\left[\frac{d\sigma}{dt}\right]_{\text{C-}N_{\text{int}}} = 2(\text{Re}f_{N_{\text{el}}}\text{Re}f_{\text{C}} + \text{Im}f_{N_{\text{el}}}\text{Im}f_{\text{C}})\cdot\frac{\pi}{k_{\text{c.m.}}^2} ,$$

where $k_{\text{c.m.}}$ is the momentum of the incident deuteron in the center-of-mass system of d-d. The phase difference between $f_{N_{\text{el}}}$ and f_{C} is important to calculate this term. We define the phase $\delta(t)$ as the difference between the pure Coulomb phase and the phase shift due to the radiative correction. It was calculated as follows:[39]

$$\delta(t) = -\frac{\alpha}{\beta}\left[\ln\left[\frac{R_d^2}{3}\right]t + C\right] ,$$

where R_d is the root-mean-square radius of the charge distribution of the deuteron and C is the Euler constant ($\approx 0.577.$) We can reevaluate the Coulomb-nuclear interference differential cross section with a pure nuclear amplitude and $\delta(t)$, where

$$f_{\text{C}} = -|f_{\text{C}}|\exp[i\delta(t)] .$$

The nuclear amplitude was assumed to be of the following form:

$$f_{N_{\text{el}}}(t) = \frac{k_{\text{c.m.}}}{4\pi}\sigma_{\text{tot}}(i+\rho)\exp(-\tfrac{1}{2}\gamma^2 t) ,$$

where σ_{tot} is the nuclear total cross section, ρ is the real-to-imaginary ratio and γ^2 is the slope parameter of d-d elastic scattering. The values of the parameters σ_{tot}, ρ, and γ^2 should be determined experimentally. They were, however, not known at this correction stage and we had to calculate their values theoretically with the Glauber model for each incident momentum. This procedure is justified because the Coulomb-nuclear interference correction is at most 0.5% of the partial cross section and the theoretical estimation of the parameters brings only a very small systematic error to the partial cross section.

E. Extrapolation

After each partial cross section was corrected as described above, the corrected data of the ith counter became

$$\sigma_{\text{tot}} - \int_0^{t_{\max}} G_i(t)\left[\left[\frac{d\sigma}{dt}\right]_{N_{\text{el}}} + \left[\frac{d\sigma}{dt}\right]_{\text{inel}}\right]dt .$$

We then assumed that the corrected cross sections were almost linear in t. It is equivalent to the assumption that $(d\sigma/dt)_{N_{\text{el}}}$ and $(d\sigma/dt)_{\text{inel}}$ fall slowly in the region where the value of $G_i(t)$ changes from unity to zero. This is a reasonable assumption in our case. Because of the above assumption, we are able to obtain the corrected cross section as a function of t_i, the momentum transfer squared corresponding to the ith counter, which is defined as

$$t_i \equiv \int_0^{t_{\max}} t\left[-\frac{d}{dt}G_i(t)\right]dt .$$

We can, therefore, approximately describe the corrected cross section of the ith counter as follows:

$$\sigma_{\text{tot}} - \int_0^{t_i}\left[\left[\frac{d\sigma}{dt}\right]_{N_{\text{el}}} + \left[\frac{d\sigma}{dt}\right]_{\text{inel}}\right]dt \equiv \sigma_{\text{corr}}(t_i) .$$

In order to obtain the total cross section σ_{tot}, we extrapolated the corrected data $[\sigma_{\text{corr}}(t_i),\ i=1,\ldots,7]$ to $t=0$ by fitting them to the form $\sigma_{\text{tot}}\exp[-At+(Bt)^2]$, where σ_{tot}, A, and B are free parameters. We took into account the covariance between the cross-section data of different counters when we consider the statistical error because of strong statistical correlation among them. The fit between the corrected data and this function was quite good. Figure 6 illustrates, as an example, the data at 4.0 GeV/c. The solid curve shows the fitted function and the open circles are the data. The cross-check data with the transmission counters covering a different t range, mentioned in Sec. II G are also shown in Fig. 6 as closed circles. The figure shows that the form of the fitting function is reasonable even at rather large angles. Each datum has an error bar, which includes the statistical and systematic errors, and is comparable to the size of the circles.

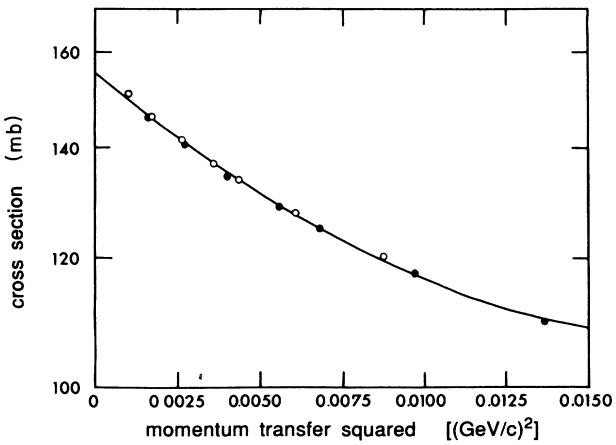

FIG. 6. Corrected partial cross-section data at 4.0 GeV/c. The solid curves show the fitted functions and the open circles are the data. The cross-check data are also shown in the figure as closed circles.

IV. RESULTS

A. Total cross sections

The d-d total cross sections are shown in Table I and Fig. 7 as a function of incident momentum. The overall error including the errors arising from the extrapolation procedure is about 0.7 mb, which is almost the same as the size of the circles of the data points in Fig. 7.

The previous experimental data are also shown in the figure. Our datum at 3.0 GeV/c totally disagrees with that by Debaisieux *et al.*,[11] but agrees quite well with that by Jaros *et al.*[13] The data by Goshaw *et al.*[12] are systematically 5 mb higher than our data around 2.0 GeV/c.

The calculated values of the cross sections are also presented in Fig. 7 by the solid, dotted, and dashed curves. The details of the calculations will be discussed in Sec. V.

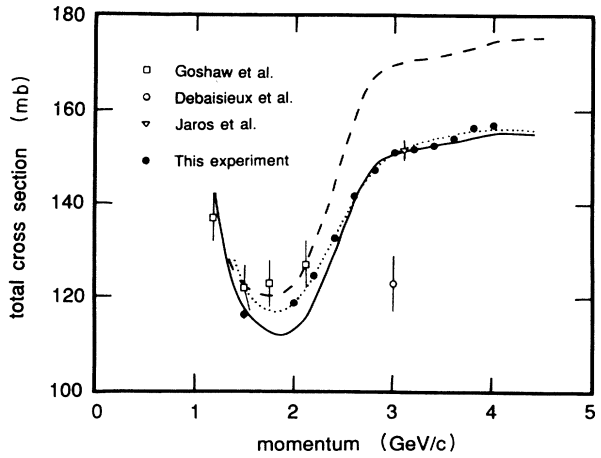

FIG. 7. Deuteron-deuteron total cross sections as a function of incident momentum. The dashed curve is the prediction of the impulse approximation, which is equal to $2\times(\sigma_{pp}+\sigma_{np})$, the solid curve is a Glauber model prediction, and the dotted curve is the prediction of a modified Glauber model calculation in which the Fermi motion of the nucleons is taken into account.

B. Error estimations

1. Random errors

In this subsection we discuss the errors that are random and statistical. There are two types of statistical errors: the counting statistics of the partial cross section σ_i and the statistical error of the momentum transfer squared t_i.

As discussed in Sec. III A, we defined the quantity M and N_i. Then N_i follows the binomial distribution. Therefore we get $\Delta N_i=[N_i(1-N_i/M)]^{1/2}$ and, accordingly,

$$\Delta\sigma_i=\frac{1}{n}\left[\left[\frac{1}{N_i}-\frac{1}{M}\right]_{\text{full}}+\left[\frac{1}{N_i}-\frac{1}{M}\right]_{\text{empty}}\right]^{1/2}.$$

We measured the partial cross sections with about a 0.5% accuracy in our experiment.

In Sec. III E we defined t_i as the momentum transfer squared corresponding to the ith counter, which can also be interpreted as the area of the acceptance function $G_i(t)$. Therefore we calculate the statistical error of the area of the histogram shown in Fig. 5. The statistical error of t_i is about 1–2 % in our experiment. This error is small and its effect on the total cross section in the extrapolation procedure is at most 0.2%.

TABLE I. Deuteron-deuteron total cross sections. The uncertainty in the cross section includes both the statistical and systematic errors.

Momentum (GeV/c)	σ_{tot} (mb)	$\Delta\sigma$ (mb)
1.5	116.30	0.92
2.0	118.77	0.77
2.2	124.74	0.66
2.4	132.71	0.77
2.6	141.70	0.71
2.8	147.42	0.76
3.0	151.13	0.73
3.2	151.81	0.71
3.4	152.41	0.74
3.6	154.08	0.74
3.8	156.63	0.71
4.0	157.13	0.73

2. Systematic errors

In this section we discuss the errors which are caused by the uncertainties in the experimental condition and our insufficient knowledge of the corrections.

As described in Sec. II B the target length was measured to an accuracy of 0.1 mm. The actual target length in the experiment was calculated as a mean of the lengths through which the extended trajectories of the incident beam traveled. After including the error caused by the misalignment of the experimental setup and the spatial resolution of the trajectories determined by the data from MWPC's, we estimated the error in the target length as at most 0.2 mm, which means that this systematic error results in the total cross section error of at most 0.1%. The effect of small bubbles on the walls of the endcaps was calculated and found to be about 0.05 mm, which is negligible. Another systematic error was caused by the uncertainty in the atmospheric pressure; it was estimated as at most 0.2% as discussed in Sec. II B. We ignore the systematic effect caused by a change in the ratio between orthodeuterium and paradeuterium because the change is very slow and cannot be observed in a few days.[40] We therefore always calculated the density of liquid deuterium as normal D_2 (ortho:para=2:1), which is in equilibrium at room temperature.

Next we discuss the errors in the correction terms. The single and multiple Coulomb correction terms are strongly dependent on the asymptotic behavior of the acceptance function $G_i(t)$ when t approaches zero. The bin width of the acceptance histogram in Fig. 5 was determined by the spatial resolution of the MWPC's and mul-

TABLE II. Values of ρ used in the calculation of the Coulomb-nuclear interference correction.

Momentum (GeV/c)	ρ
1.5	0.556
2.0	0.221
2.2	0.169
2.4	0.110
2.6	0.038
2.8	−0.051
3.0	−0.130
3.2	−0.185
3.4	−0.219
3.6	−0.240
3.8	−0.252
4.0	−0.257

tiple scattering by air. Therefore we cannot determine the difference between the function $G_i(t)$ and the real acceptance to an accuracy less than the bin width of 1.25×10^{-4} (GeV/c)^2. We calculated the corrections by using the function $G_i(t)$ and by using the discrete values of the acceptance histogram itself. From the comparison of the two results, a systematic error of multiple Coulomb scattering was estimated to be 60% and that of single Coulomb scattering to be 15% for the smallest counter. On the other hand, the Coulomb-nuclear interference term is weakly dependent on the acceptance function. The systematic error of this correction term is caused mainly by the uncertainties of the parameters determined with the Glauber model (see Sec. III D). First, we assumed the uncertainties of the parameters of the N-N amplitude as follows: $\Delta\sigma_{pp}=\pm0.25$ mb, $\Delta\sigma_{np}=\pm0.3$ mb, $\Delta\rho_{pp}=\pm0.05$, $\Delta\rho_{np}=\pm0.05$, $\Delta\gamma^2_{pp}=\pm0.3$ (GeV/c)$^{-2}$, and $\Delta\gamma^2_{np}=\pm0.4$ (GeV/c)$^{-2}$. The uncertainties propagate into the systematic errors of the parameters of the d-d amplitude, $\sigma_{\rm tot}$, ρ, and γ^2. We estimated these errors and found that the systematic error in ρ was important for the evaluation of the systematic error in the Coulomb-nuclear interference correction, while the effects of the errors in $\sigma_{\rm tot}$ and γ^2 on the correction were negligible. The error in ρ was estimated to be ±0.035 for the d-d amplitude, which corresponds to a total cross section error of about 0.1 mb. Therefore we determined the systematic error of the Coulomb-nuclear interference as $(3.5/\rho)\%$, where ρ is the calculated values. The values of ρ we used are tabulated in Table II.

The systematic errors in the momentum transfer squared t_i are caused by the uncertainty in the acceptance function and the uncertainties of the experimental setup of the MWPC's. We carefully estimated the overall error and found it to be 2–3 %. It is about the same as the statistical error and the effect on the total cross section is about 0.2%.

V. THEORETICAL CALCULATIONS AND DISCUSSIONS

A. Glauber model calculations

Deuteron-deuteron scattering is the simplest example of nucleus-nucleus scattering. Hence the Glauber calculation of the d-d amplitude can be performed rather exactly. But we calculated the amplitude using the N-N amplitude with no spin dependence for the simplicity of the calculation of the multiple scattering terms. On the other hand, the isospin dependence can be taken into account easily.

Consequently, the d-d amplitude becomes the following:[3]

$$
\begin{aligned}
F_{dd}(\mathbf{q})=&\,8S^2(\mathbf{q}/2)f(\mathbf{q})+\frac{8i}{\pi k}S(\mathbf{q}/2)\int d^2\mathbf{Q}'S(\mathbf{Q}')[f(\mathbf{q}/2+\mathbf{Q}')f(\mathbf{q}/2-\mathbf{Q}')-3g(\mathbf{q}/2+\mathbf{Q}')g(\mathbf{q}/2-\mathbf{Q}')]\\
&+\frac{4i}{\pi k}\int d^2\mathbf{Q}'S^2(\mathbf{Q}')[f(\mathbf{q}/2+\mathbf{Q}')f(\mathbf{q}/2-\mathbf{Q}')+3g(\mathbf{q}/2+\mathbf{Q}')g(\mathbf{q}/2-\mathbf{Q}')]\\
&-\frac{8}{\pi^2k^2}\int d^2\mathbf{Q}'d^2\mathbf{Q}''S(\mathbf{Q}')S(\mathbf{Q}'')\\
&\quad\times[f(\mathbf{Q}'+\mathbf{Q}'')f(\mathbf{q}/2-\mathbf{Q}'')f(\mathbf{q}/2-\mathbf{Q}')-6g(\mathbf{Q}'+\mathbf{Q}'')g(\mathbf{q}/2-\mathbf{Q}'')f(\mathbf{q}/2-\mathbf{Q}')\\
&\quad+3f(\mathbf{Q}'+\mathbf{Q}'')g(\mathbf{q}/2-\mathbf{Q}'')g(\mathbf{q}/2-\mathbf{Q}')]\\
&-\frac{2i}{\pi^3k^3}\int d^2\mathbf{Q}'d^2\mathbf{Q}''d^2\mathbf{Q}'''S(\mathbf{Q}'')S(\mathbf{Q}''')\\
&\quad\times[f(\mathbf{Q}')f(\mathbf{q}/2-\mathbf{Q}'-\mathbf{Q}'')f(\mathbf{q}/2-\mathbf{Q}'-\mathbf{Q}''')f(\mathbf{Q}'+\mathbf{Q}''+\mathbf{Q}''')\\
&\quad-12g(\mathbf{Q}')g(\mathbf{q}/2-\mathbf{Q}'-\mathbf{Q}'')f(\mathbf{q}/2-\mathbf{Q}'-\mathbf{Q}''')f(\mathbf{Q}'+\mathbf{Q}''+\mathbf{Q}''')\\
&\quad+6g(\mathbf{Q}')f(\mathbf{q}/2-\mathbf{Q}'-\mathbf{Q}'')f(\mathbf{q}/2-\mathbf{Q}'-\mathbf{Q}''')g(\mathbf{Q}'+\mathbf{Q}''+\mathbf{Q}''')\\
&\quad+21g(\mathbf{Q}')g(\mathbf{q}/2-\mathbf{Q}'-\mathbf{Q}'')g(\mathbf{q}/2-\mathbf{Q}-\mathbf{Q}''')g(\mathbf{Q}'+\mathbf{Q}''+\mathbf{Q}''')],
\end{aligned}
$$

where

$$f(\mathbf{q})=[f_{pp}(k/2,\mathbf{q})+f_{np}(k/2,\mathbf{q})]/2 ,$$

$$g(\mathbf{q})=[f_{pp}(k/2,\mathbf{q})-f_{np}(k/2,\mathbf{q})]/2 ,$$

and k is the incident momentum of the deuteron. When we calculate the total cross sections with unpolarized beams, the form factor $S(\mathbf{q})$ can be reduced as

$$S(\mathbf{q})=\int \exp(i\mathbf{q}\cdot\mathbf{r})|\Psi(\mathbf{r})|^2 d\mathbf{r} ,$$

where $\Psi(\mathbf{r})$ is the configuration-space wave function of the deuteron ground state and $\mathbf{r}$ is the relative coordinate of one constituent nucleon with respect to the other nucleon. We used the deuteron wave function based on the Paris potential and the spin-independent N-N amplitude in the calculation. We approximated the N-N amplitude as

$$f_{NN}(k,\mathbf{q})=\frac{k}{4\pi}\sigma_{NN}(i+\rho_{NN})\left[R\exp\left[-\frac{a}{2}q^2\right]+(1-R)\exp\left[-\frac{b}{2}q^2\right]\right] \quad (NN=pp,np) ,$$

where σ_{NN} and ρ_{NN} are the nucleon-nucleon total cross section and real-to-imaginary ratio of the amplitudes, respectively. We determined the values of the parameters a, b, and R by fitting the data from the phase shift analysis by Arndt, Hyslop, and Roper[18] to the above formula. This double-slope amplitude was adopted since it reproduced the phase-shift data better than a single-slope amplitude.

The calculated amplitude of d-d scattering was used for the Coulomb-nuclear interference correction and the comparison with our experimental total cross sections. The result of the Glauber calculation of the d-d total cross section is uncertain to ± 0.9 mb, which is due mainly to the uncertainties in the nucleon-nucleon parameters.

B. Discussions

1. *Effect of Fermi motion*

Our d-d total cross-sections data and the results of the Glauber calculation are shown in Fig. 7. The dashed curves represent the impulse approximation prediction $2\times(\sigma_{pp}+\sigma_{np})$, which is based on the assumption that the d-d amplitude can be described as the sum of the N-N amplitudes, and the solid curve represents the Glauber model prediction. The data and the Glauber model calculation are in good agreement above 2.6 GeV/c. But the data are higher than the Glauber calculation and lower than the impulse approximation prediction around 2.0 GeV/c, where the cross section dips.

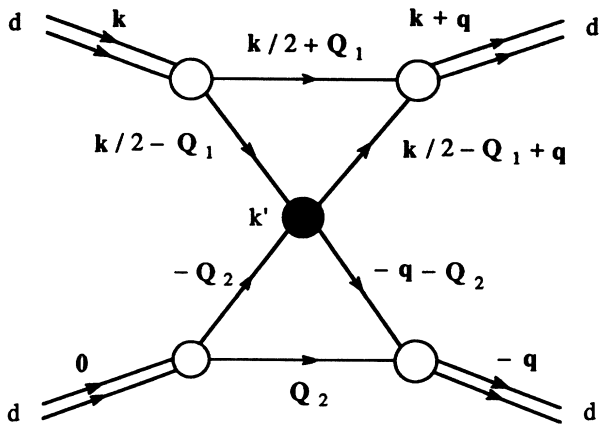

FIG. 8. Schematic diagrams of the single scattering process of d-d elastic scattering.

To see if a more refined calculation might remove this discrepancy, we redid the calculation by including the effect of the Fermi motion of the nucleons in the deuteron, which is neglected in the Glauber model calculations. For example, Fig. 8 shows a diagram of d-d elastic scattering. The closed circles represent the scattering process and correspond to the scattering amplitude $f(\mathbf{q})$, while the open circles represent the initial and final bound states of the deuteron and correspond to the momentum-space wave function $\phi(\mathbf{Q})$. Then, the single scattering term becomes proportional to

$$\int d^3\mathbf{Q}_1 d^3\mathbf{Q}_2 \phi^\dagger(\mathbf{Q}_2+\mathbf{q}/2)\times\phi^\dagger(\mathbf{Q}_1-\mathbf{q}/2) f(k',\mathbf{q})\phi(\mathbf{Q}_1)\phi(\mathbf{Q}_2) ,$$

where k' is the momentum of the incident nucleon in the rest frame of the target nucleon in the deuteron, and $\mathbf{Q}_1$ and $\mathbf{Q}_2$ are the momenta due to Fermi motion (Fermi momenta). If we assume that the amplitude $f(k',\mathbf{q})$ is independent of the Fermi momenta (e.g., $k'=|\mathbf{k}|/2$), this integration becomes

$$f(k/2,\mathbf{q})\int d^3\mathbf{Q}_1\phi^\dagger(\mathbf{Q}_1-\mathbf{q}/2)\phi(\mathbf{Q}_1)\int d^3\mathbf{Q}_2\phi^\dagger(\mathbf{Q}_2+\mathbf{q}/2)\phi(\mathbf{Q}_2)=f(k/2,\mathbf{q})S^2(\mathbf{q}/2) .$$

This is the single scattering term of the Glauber amplitude. In the same way, the double scattering term can be described as the integration with respect to the Fermi momenta, and if the amplitudes are independent of the Fermi momenta, we can obtain the double scattering term of the Glauber amplitude. (The details of this method are described by Wilkin in the case of p-d scattering.[41])

In order to include the effect of Fermi motion, we recover the integration of the amplitude $f(k',\mathbf{q})$ with respect to the Fermi momenta $\mathbf{Q}_1$ and $\mathbf{Q}_2$ in the calculation. For simplicity of calculation, we consider only the

impulse approximation (IA) term (e.g., the single scattering term) of d-d scattering. The amplitude of this term becomes

$$F_{\mathrm{IA}}(\mathbf{q})=8\int d^3\mathbf{Q}_1 d^3\mathbf{Q}_2 \phi^{\dagger}(\mathbf{Q}_2+\mathbf{q}/2)\phi^{\dagger}(\mathbf{Q}_1-\mathbf{q}/2) \times f(k',\mathbf{q})\phi(\mathbf{Q}_1)\phi(\mathbf{Q}_2)\ .$$

Then, the total cross section is obtained with the aid of the optical theorem

$$\sigma_{\mathrm{IA}}=\frac{4\pi}{k}\mathrm{Im}F_{\mathrm{IA}}(\mathbf{0}) =\int d^3\mathbf{Q}_1 d^3\mathbf{Q}_2 \frac{2k'}{k}\sigma_G(k')|\phi(\mathbf{Q}_1)|^2\cdot|\phi(\mathbf{Q}_2)|^2\ ,$$

where k is the momentum of the incident deuteron in the rest frame of the deuteron center of mass, k' is that of the incident nucleon in the rest frame of the scattering nucleon in the deuteron, and $\sigma_G(k')$ is the d-d total cross section calculated with the impulse approximation term of the Glauber calculation. This result shows the fact that the Glauber predicted total cross section must be smeared with Fermi momenta $\mathbf{Q}_1$ and $\mathbf{Q}_2$ which follow the momentum distribution of the deuteron $|\phi(\mathbf{Q}_1)|^2$. The effect of Fermi motion is larger in the case of d-d scattering than in the case of p-d scattering because both the projectile and target nucleons have Fermi motion in d-d scattering. We approximate the theoretical value of the d-d total cross section including Fermi motion as

$$\sigma_{dd}=\sigma_{\mathrm{IA}}-\Delta\sigma_D\ ,$$

where $\Delta\sigma_D$ is the cross-section defect due to the multiple-scattering terms of the Glauber calculation. The effect of Fermi motion on the multiple-scattering terms is ignored because the multiple-scattering terms including the effect of Fermi motion never reduce to a simple form. This procedure is justified because the cross-section defect is only 10% of the total cross section in the d-d scattering case, and its energy dependence is moderate compared with that of the impulse approximation term.

The result of this calculation is shown as the dotted curve in Fig. 7. The effect of Fermi motion smears the theoretical curve predicted by the Glauber model, particularly around 2.0 GeV/c. It clearly shows a better agreement than before in the whole of our momentum range except for the datum at 1.5 GeV/c. An important point is that the Glauber model corrected for Fermi motion agrees with our experimental data even in the low-momentum region where the angular distribution of p-p scattering is nearly flat, and where Goshaw *et al.*[12] claimed an agreement with the impulse approximation. The effect of Fermi motion is large in the region where the parameters of the scattering amplitude have a strong energy dependence. Therefore we must, at first, take into account of Fermi motion in such region before claiming that the validity of the Glauber model is limited. Even though the better agreement with the inclusion of the effect of Fermi motion comes as no surprise, we wish to stress that we were able to meaningfully calculate this effect for the first time because our experiment was a high precision one covering a large range of energy. For example, the data by Goshaw *et al.* and Debaisieux *et al.* have insufficient accuracy for this purpose, and the datum by Jaros *et al.* is only for a single point where the effect of Fermi motion is very small.

As a further check of the effect of the inclusion of Fermi momentum we also investigated the p-d total cross section data by calculating p-d total cross sections in the same way as described above. Figure 9 shows various p-d total cross-section data[14–17] together with the results of (a) a standard Glauber model calculation (solid curve), (b) the refined Glauber model calculation (dotted curve), and (c) the impulse approximation model (dashed curve). Even though an agreement between the experimental data and the impulse approximation has been claimed in the case of p-d total cross section, the agreement is fortuitous, and the Glauber model with Fermi motion seems to most adequately describe p-d scattering as well. The effect of Fermi motion on the π-d total cross section has been calculated by Fäldt and Ericson.[42] They also obtained quantitative agreement between the calculation and the experimental data, and claimed that the single scattering term must be smeared by the Fermi momentum in the resonance region and that the effect on the multiple scattering term is relatively small. Besides the effect of smearing, some other effects of Fermi motion have been discussed by several authors.[43–45] However, only the effect of smearing is significant enough to explain the experimental data in our energy region, where the total cross-section data are strongly dependent on energy.

2. *Other effects*

Though the Glauber model calculation including the effect of Fermi motion agrees fairly well with our data on the d-d total cross section, there is some disagreement still at 1.5 GeV/c. In addition, p-^{4}He, p-C, and p-O total

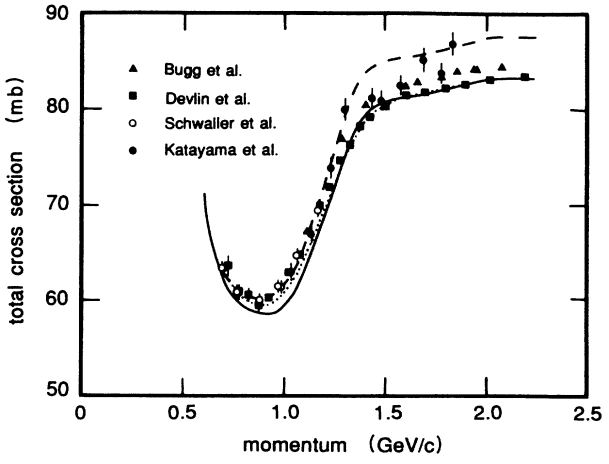

FIG. 9. Proton-deuteron total cross sections as a function of incident proton momentum. The dashed curve is the prediction of the impulse approximation, which is equal to $\sigma_{pp}+\sigma_{np}$, the solid curve is a Glauber model prediction, and the dotted curve is the prediction of a modified Glauber model calculation in which the Fermi motion of the nucleons is taken into account.

cross section data[16] seem to disagree with the calculation even after including the effect of Fermi motion below 1.0 GeV/c per nucleon, where the p-d total cross section data still agree with such calculation. Therefore, in this subsection, we briefly summarize the possible effects to affect the calculated values of the total cross section and suggest clues for future improvements.

First, we consider the N-N amplitude. In the calculation of the d-d amplitude, we neglected the spin dependence of the N-N amplitude. The spin contributions to the amplitude at small angles rapidly decrease with increasing incident momentum and become close to zero at about 1.2 GeV/c per nucleon.[46] Therefore the effect of the spin is probably small in the high-momentum region, while the neglect of the spin effect is no longer justified in the region below 1.0 GeV/c per nucleon. Furthermore, the spin contribution to the total cross section seems to become larger with the increase in the number of nucleons in the reaction because this contribution to the forward elastic amplitude appears in the multiple-scattering terms. For example, by including the spin dependence, the theoretical value of p-d total cross section at 1.7 GeV/c changes by about 0.3%, while that of p-^{4}He total cross section by about 4%.[47]

Next, we consider corrections to the Glauber theory. One of them is the effect of Fermi motion discussed in the previous subsection. Another correction is, for example, the contribution of backward N-N scattering. This can be taken into account by including the diagrams of backward N-N scattering or N-N scattering between the nucleons in the same nucleus. These diagrams are ignored in the Glauber calculation. However, their contribution to nucleus-nucleus forward elastic scattering seems to be very small in our energy region because a large momentum transfer to a nucleon in the nuclei usually induces a breakup reaction.

VI. CONCLUSIONS

The d-d total cross sections have been obtained with high accuracy in the incident deuteron momentum range 1.5–4.0 GeV/c. This measurement is the first systematic investigation of the energy dependence of d-d total cross sections in the intermediate-energy region.

The results are in good agreement with the prediction by the Glauber model over the entire momentum range, and there is no anomalous structure in the energy dependence of the total cross section. In particular, the d-d total cross section data above 2.0 GeV/c agree quite well with a modified Glauber calculation which includes the effect of the Fermi motion of the nucleons in the deuteron. Such comparison is only possible with a set of precise data over a wide energy range such as ours.

ACKNOWLEDGMENTS

We are grateful to the operating crews of the National Laboratory for High Energy Physics proton synchrotron (KEK PS), beam channel, and cryogenic groups for their assistance during the experiment. We wish to thank Prof. T. Nishikawa and the administrative staff of the KEK Physics Department for their assistance and cooperation. We also thank Dr. N. Katayama and Mr. T. Mizusaki for their help and fruitful discussion on the Glauber calculation. The computation for this work was performed at the KEK Computer Center and the Meson Science Laboratory of University of Tokyo.

---

*Present address: IBM Research, Tokyo Research Laboratory, Sanbancho, Chiyoda-ku, Tokyo 102, Japan.

†Present address: Elionics Ltd., Hachioji, Tokyo 192, Japan.

[1]R. J. Glauber, in *Lectures in Theoretical Physics*, edited by W. E. Brittin and L. G. Dunham (Interscience, New York, 1959), Vol. I, p. 315.

[2]V. Franco and R. J. Glauber, Phys. Rev. **142**, 1195 (1966).

[3]V. Franco, Phys. Rev. **175**, 1376 (1968).

[4]W. Czyż and L. C. Maximon, Ann. Phys. (N.Y.) **52**, 59 (1969).

[5]A. Tékou, Nucl. Phys. **B46**, 152 (1972).

[6]G. D. Alkhazov *et al.*, Nucl. Phys. **A280**, 365 (1977).

[7]V. Franco and G. K. Varma, Phys. Rev. C **15**, 1375 (1977).

[8]V. Franco and G. K. Varma, Phys. Rev. C **18**, 349 (1978).

[9]G. Fäldt and H. Pilkuhn, Ann. Phys. (N.Y.) **58**, 454 (1970).

[10]G. Fäldt and I. Hulthage, Nucl. Phys. **A316**, 253 (1979).

[11]J. Debaisieux, F. Grard, J. Heughebaert, R. Servranckx, and R. Windmolders, Nucl. Phys. **70**, 603 (1965).

[12]A. T. Goshaw, P. J. Oddone, M. J. Bazin, and C. R. Sun, Phys. Rev. Lett. **23**, 990 (1969).

[13]J. Jaros *et al.*, Phys. Rev. C **18**, 2273 (1978).

[14]D. V. Bugg, D. C. Salter, G. H. Stafford, R. F. George, K. F. Riley, and R. J. Tapper, Phys. Rev. **146**, 980 (1966).

[15]T. J. Devlin, W. Johnson, J. Norem, K. Vosburgh, R. E. Mischke, and W. Schimmerling, Phys. Rev. D **8**, 136 (1973).

[16]P. S. Schwaller, M. Pepin, B. Favier, C. Richard-Serre, D. F. Measday, and P. U. Renberg, Nucl. Phys. **A316**, 317 (1979).

[17]N. Katayama, F. Sai, T. Tsuboyama, and S. S. Yamamoto, Nucl. Phys. **A438**, 685 (1985).

[18]R. A. Arndt, J. S. Hyslop III, and L. D. Roper, Phys. Rev. D **35**, 128 (1987).

[19]A. T. Goshaw, P. J. Oddone, M. J. Bazin, and C. R. Sun, Phys. Rev. Lett. **25**, 249 (1970).

[20]V. Franco and Y. Yin, Phys. Rev. C **34**, 608 (1986).

[21]G. D. Alkhazov, Nucl. Phys. **A280**, 330 (1977).

[22]T. Sumiyoshi, S. Suzuki, and K. Nakamura, Jpn. J. Appl. Phys. **22**, 1606 (1983).

[23]K. Ishikawa, T. Kishida, M. Kuze, F. Sai, T. Tsuboyama, S. S. Yamamoto, and T. Maki, Nucl. Instrum. Methods **A270**, 6 (1988).

[24]K. Ishikawa, T. Kishida, M. Kuze, F. Sai, T. Tsuboyama, S. S. Yamamoto, T. Maki, and S. Suzuki, Jpn. J. Appl. Phys. **28**, 495 (1989).

[25]E. R. Grilly, J. Am. Chem. Soc. **73**, 843 (1951).

[26]E. C. Kerr, J. Am. Chem. Soc. **74**, 824 (1952).

[27]F. Sai, N. Katayama, T. Tsuboyama, and S. S. Yamamoto, Phys. Rev. Lett. **55**, 2668 (1985).
[28]M. Kuze, K. Ishikawa, T. Kishida, F. Sai, T. Tsuboyama, and S. S. Yamamoto, Jpn. J. Appl. Phys. **26**, 1348 (1987).
[29]V. Amaldi *et al.*, Nuovo Cimento **46A**, 171 (1962).
[30]G. Giacomelli, in *Progress in Nuclear Physics,* edited by D. M. Brink and J. H. Mulvey (Pergamon, New York, 1970), Vol. 12, p. 77.
[31]P. S. Schwaller, B. Favier, D. F. Measday, M. Pepin, P. U. Renberg, and C. Serre, CERN Report 72-13, 1972.
[32]M. Lacombe, B. Loiseau, J. M. Richard, R. Vinh Mau, J. Côté, P. Pirés, and R. de Tourreil, Phys. Rev. C **21**, 861 (1980).
[33]M. Lacombe, B. Loiseau, R. Vinh Mau, J. Côté, P. Pirés, and R. de Tourreil, Phys. Lett. **101B**, 139 (1981).
[34]H. A. Bethe, Phys. Rev. **89**, 1256 (1953).
[35]A. M. Cormack, Nucl. Phys. **52**, 286 (1964).
[36]G. Molière, Z. Naturforsch. **3a**, 78 (1948).
[37]H. Øverås, CERN Report 63-9, 1963.
[38]U. Fano, Phys. Rev. **93**, 121 (1954).
[39]M. P. Locher, Nucl. Phys. **B2**, 525 (1967).
[40]H. W. Woolley, R. B. Scott, and F. G. Brickwedde, J. Res. Natl. Bur. Stand. **41** 379 (1948).
[41]C. Wilkin, in *Nuclear and Particle Physics,* edited by B. Margolis and C. S. Lam (Benjamin, New York, 1968), p. 439.
[42]G. Fäldt and T. E. O. Ericson, Nucl. Phys. **B8**, 1 (1968).
[43]G. B. West, Ann. Phys. (N.Y.) **74**, 464 (1972).
[44]S. J. Wallace, Phys. Rev. C **12**, 179 (1975).
[45]D. Kusno and M. J. Moravcsik, Phys. Rev. D **20**, 2734 (1979).
[46]G. D. Alkhazov, S. L. Belostotsky, and A. A. Vorobyov, Phys. Rep. **42C**, 89 (1978).
[47]V. Franco, Phys. Rev. Lett. **21**, 1360 (1968).